GIRK3 gates activation of the mesolimbic dopaminergic pathway by ethanol

Melissa A. Herman[a], Harpreet Sidhu[a], David G. Stouffer[a], Max Kreifeldt[a], David Le[a], Chelsea Cates-Gatto[b], Michaelanne B. Munoz[c], Amanda J. Roberts[b], Loren H. Parsons[a], Marisa Roberto[a], Kevin Wickman[d], Paul A. Slesinger[c,e], and Candice Contet[a,1]

[a]Committee on the Neurobiology of Addictive Disorders, The Scripps Research Institute, La Jolla, CA 92037; [b]Department of Molecular and Cellular Neuroscience, The Scripps Research Institute, La Jolla, CA 92037; [c]Clayton Foundation Laboratories for Peptide Biology, The Salk Institute for Biological Studies, La Jolla, CA 92037; [d]Department of Pharmacology, University of Minnesota, Minneapolis, MN 55455; and [e]Department of Neuroscience, Icahn School of Medicine at Mount Sinai, New York, NY 10029

Edited* by Floyd Bloom, The Scripps Research Institute, La Jolla, CA, and approved April 9, 2015 (received for review August 21, 2014)

G protein-gated inwardly rectifying potassium (GIRK) channels are critical regulators of neuronal excitability and can be directly activated by ethanol. Constitutive deletion of the GIRK3 subunit has minimal phenotypic consequences, except in response to drugs of abuse. Here we investigated how the GIRK3 subunit contributes to the cellular and behavioral effects of ethanol, as well as to voluntary ethanol consumption. We found that constitutive deletion of GIRK3 in knockout (KO) mice selectively increased ethanol binge-like drinking, without affecting ethanol metabolism, sensitivity to ethanol intoxication, or continuous-access drinking. Virally mediated expression of GIRK3 in the ventral tegmental area (VTA) reversed the phenotype of GIRK3 KO mice and further decreased the intake of their wild-type counterparts. In addition, GIRK3 KO mice showed a blunted response of the mesolimbic dopaminergic (DA) pathway to ethanol, as assessed by ethanol-induced excitation of VTA neurons and DA release in the nucleus accumbens. These findings support the notion that the subunit composition of VTA GIRK channels is a critical determinant of DA neuron sensitivity to drugs of abuse. Furthermore, our study reveals the behavioral impact of this cellular effect, whereby the level of GIRK3 expression in the VTA tunes ethanol intake under binge-type conditions: the more GIRK3, the less ethanol drinking.

Kir3.3 | Kcnj9 | alcohol | reward | ventral midbrain

G protein-gated inwardly rectifying potassium (GIRK) channels mediate slow inhibitory postsynaptic potentials following activation of $G_{i/o}$-coupled receptors, thereby regulating membrane excitability in neuronal, cardiac, and endocrine cells. In neurons, GIRK channels exist as GIRK2 homotetramers or heterotetramers of GIRK1, GIRK2, and/or GIRK3 (reviewed in ref. 1). Despite overlapping distributions in the central nervous system, the three subunits exhibit cell type-specific patterns of expression within some brain regions (2–7). In particular, in the ventral tegmental area (VTA), dopaminergic (DA) neurons express only GIRK2 and GIRK3, whereas non-DA neurons also express GIRK1, a discrepancy that drives differential sensitivity of the two cell populations to $G_{i/o}$-coupled receptor (e.g., $GABA_B$ receptor) activation (8–10).

In addition to their activation by $G_{i/o}$-coupled receptors, GIRK channels also can be directly activated by ethanol (11–14). The behavioral significance of GIRK channel activation by ethanol (either directly or through G proteins) is poorly understood, however. GIRK2 knockout (KO) mice are less sensitive to ethanol's rewarding and aversive effects, as measured in conditioned place preference and conditioned taste aversion tests (15). Ethanol-induced locomotor stimulation, anxiolytic-like effect, and withdrawal severity are also blunted in the absence of GIRK2 (16). Constitutive GIRK2 deletion produces numerous behavioral abnormalities, however, including increased seizure susceptibility, reduced anxiety-like behavior, hyperactivity, hyperalgesia, and enhanced operant response for food, making it difficult to interpret the effects of ethanol in GIRK2 KO mice (reviewed in ref. 17). In contrast, GIRK3 KO mice are indistinguishable from wild-type (WT) mice in many behavioral assays (e.g., locomotor activity, anxiety-like behavior, motor balance, response for food), suggesting that GIRK3 subunits contribute in a more subtle manner to the function of GIRK channels in vivo (18, 19); however, GIRK3 KO mice exhibit reduced response for cocaine self-administration and blunted hyperexcitability during withdrawal from sedative-hypnotic drugs, suggesting that GIRK3 plays an important role in the neuronal activity and plasticity evoked by drugs of abuse (20, 21).

In the present study, we examined the contribution of GIRK3 to the cellular and behavioral effects of ethanol, as well as to ethanol consumption. We show that GIRK3 in VTA neurons is essential for the activation of the mesolimbic DA system by ethanol, and that it selectively modulates binge-like drinking without influencing behavioral manifestations of ethanol intoxication. Our findings support the notion that the subunit composition of VTA GIRK channels is a critical determinant of DA neuron sensitivity to drugs of abuse (9, 10, 22).

Results

GIRK3 Deletion Does Not Alter Ethanol Metabolism and Intoxication, but Reduces Withdrawal-Induced Hyperexcitability. We assessed whether the absence of GIRK3 alters ethanol metabolism by measuring blood alcohol level (BAL) over the course of 4 h after the i.p. injection of 2 g/kg ethanol in WT and GIRK3 KO mice (cohort 1; Fig. 1 *A* and *B*). BAL was negatively correlated with time in both WT ($R^2 = 0.98$; $P \leq 0.001$) and GIRK3 KO ($R^2 = 0.98$; $P \leq 0.001$) mice, and there was no effect of genotype [$F_{1,6} = 0.89$; *P*, not significant (n.s.)] and no interaction between time and genotype ($F_{3,18} = 0.83$; *P*, n.s.).

Significance

G protein-gated inwardly rectifying potassium (GIRK) channels regulate neuronal excitability and can be activated by ethanol. The role of GIRK channels in the behavioral effects of ethanol is poorly understood, however. This study shows that genetic ablation of GIRK3, one of four GIRK subunits, prevents ethanol from activating the mesolimbic dopaminergic pathway, a neuronal circuit subserving the motivation to seek reward (incentive salience), and enhances binge-like drinking. Conversely, increasing GIRK3 expression in the ventral midbrain, where this pathway originates, reduces binge-like drinking. Thus, GIRK3 appears to be a critical gatekeeper of ethanol incentive salience and a potential target for the treatment of excessive ethanol consumption.

Author contributions: A.J.R., L.H.P., M.R., and C.C. designed research; M.A.H., H.S., D.G.S., M.K., D.L., C.C.-G., M.B.M., and C.C. performed research; K.W. and P.A.S. contributed new reagents/analytic tools; M.A.H., H.S., and C.C. analyzed data; and C.C. wrote the paper.

The authors declare no conflict of interest.

*This Direct Submission article had a prearranged editor.

[1]To whom correspondence should be addressed. Email: contet@scripps.edu.

This article contains supporting information online at www.pnas.org/lookup/suppl/doi:10.1073/pnas.1416146112/-/DCSupplemental.

We then evaluated the impact of GIRK3 deletion on the sensitivity to acute ethanol exposure by comparing WT and GIRK3 KO mice in a series of behavioral tests (cohort 2; Fig. 1*A*). Ethanol (1.5 g/kg i.p.) reduced the ability of the mice to stay on a rotating rod ($F_{1,28} = 14.6$; $P \leq 0.001$) to the same extent in WT and GIRK3 KO mice ($F_{1,28} = 0.3$; *P*, n.s.) (Fig. 1*C*). Likewise, the duration of ethanol (4 g/kg i.p.)-induced loss-of-righting reflex and BAL at recovery were not affected by GIRK3 deletion ($t_{12} = -0.4$; *P*, n.s. and $t_{12} = 0.4$; *P*, n.s., respectively) (Fig. 1*D*).

WT and GIRK3 KO mice did not differ in baseline body temperature ($t_{30} = -0.5$; *P*, n.s.) or the hypothermic effect of ethanol (4 g/kg, i.p.; $F_{1,28} = 332.2$; $P \leq 0.001$) was insensitive to the absence of GIRK3 ($F_{1,28} = 0.001$; *P*, n.s.) (Fig. 1*E*). In contrast, handling-induced convulsions (HICs), which peaked at 8 h into withdrawal in the WT mice (saline vs. ethanol, $U_{14} = 13.5$; $P \leq 0.05$), were abolished in KO mice (saline vs. ethanol: $U_{14} = 30.0$; *P*, n.s.; WT vs. KO: $U_{14} = 15$; $P \leq 0.05$) (Fig. 1*F*). The latter finding is consistent with a previous report showing that GIRK3 KO mice backcrossed on a DBA/2J background experience less severe withdrawal from sedative-hypnotic drugs (including ethanol) compared with their WT counterparts (20). Both genotypes were equally sensitive to the initial sedative effect of ethanol (at 2 h: WT, $U_{14} = 10.5$; $P \leq 0.01$; KO, $U_{14} = 4.5$; $P \leq 0.001$; at 4 h: WT, $U_{14} = 14$, $P \leq 0.05$; KO, $U_{14} = 11.5$, $P \leq 0.05$; no significant difference between genotypes at either time point), in accordance with the findings of the loss of righting reflex experiment.

GIRK3 in the VTA Moderates Binge-Like Drinking. We next examined whether the absence of GIRK3 affects voluntary ethanol drinking (Fig. 2*A*). When given limited access to ethanol (2-h two-bottle choice; cohort 3), GIRK3 KO mice consumed more ethanol than their WT counterparts ($t_{28} = 3.7$; $P \leq 0.001$) (Fig. 2*B*). Under these experimental conditions, water intake was very limited in both genotypes, thereby precluding the detection of a potential genotype effect on ethanol preference ($t_{28} = 0.5$; *P*, n.s.) (Fig. 2*B*). A different group of WT and KO mice (cohort 4) was given continuous access to ethanol, and the two genotypes stabilized their intake at similar levels ($t_{38} = 0.1$; *P*, n.s.), with equivalent selectivity for the ethanol solution ($t_{38} = -0.2$; *P*, n.s.) (Fig. 2*C*). However, when the same mice were then offered limited access to a single bottle of ethanol (4-h sessions), an effect of genotype again became evident, with KO mice drinking more ethanol than WT mice, particularly during the early phase of the session (0–2 h: $t_{38} = 2.6$; $P \leq 0.01$; 2–4 h: $t_{38} = 1.4$; *P*, n.s.; 0–4 h: $t_{38} = 2.6$; $P \leq 0.01$) (Fig. 2*D*). Taken together, these results suggest that GIRK3 subunits exert an inhibitory influence on binge-like drinking.

GIRK3 subunits are expressed throughout the central nervous system (2), making it difficult to ascribe the effect of GIRK3 deletion on binge-like drinking to a particular brain region. GIRK2/3 channels in VTA DA neurons recently have been implicated in regulating the sensitivity to γ-hydroxybutyrate (GHB) and cocaine (9, 10, 22), however, suggesting a potential neuroanatomical substrate mediating the role of GIRK3 in ethanol drinking. To examine this possibility, we injected mice with a lentiviral (LV) vector expressing either YFP-GIRK3 or GFP (negative control) in the VTA (cohort 4; Fig. 2*F*). As expected from the broad tropism of LV vectors and the CaMKII promoter driving transgene expression, the reporters (YFP/GFP) were detected in both DA [tyrosine hydroxylase (TH)-positive] and non-DA (TH-negative) cells (Fig. 2*G*). Expression of YFP-GIRK3, but not of GFP alone, in the VTA of GIRK3 KO mice restored ethanol intake to WT levels (Fig. 2*E*). Specifically, virally mediated expression of GIRK3 in the VTA lowered ethanol intake in both genotypes in the early phase of the drinking session (Fig. 2*E*), as reflected by a vector effect (0–2 h: $F_{1,28} = 4.5$; $P \leq 0.05$; 2–4 h: $F_{1,28} = 0.8$; *P*, n.s.; 0–4 h: $F_{1,28} = 3.7$; $P = 0.07$) and the lack of a vector × genotype interaction (0–2 h: $F_{1,28} = 0.02$; *P*, n.s.; 2–4 h: $F_{1,28} = 0.08$; *P*, n.s.; 0–4 h: $F_{1,28} = 0.05$; *P*, n.s.). The effect of genotype was no longer significant after injection of the vectors (0–2 h: $F_{1,28} = 2.7$; *P*, n.s.; 0–4 h: $F_{1,28} = 3.7$; $P = 0.07$). Thus, the level of GIRK3 expression in the VTA appears to determine ethanol consumption under binge-type conditions, raising the possibility that GIRK3 modulates the response of the mesolimbic DA pathway to ethanol.

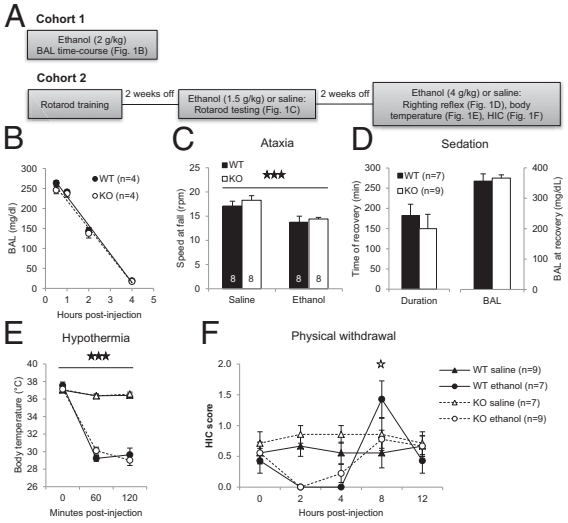

Fig. 1. Ethanol-induced ataxia, sedation, hypothermia, and withdrawal hyperexcitability in WT and GIRK3 KO mice. (*A*) Testing timeline for results presented in *B*–*F*. (*B*) Mice were injected with ethanol (2 g/kg i.p.), and the time course of ethanol clearance was determined by repeatedly measuring BAL. (*C*). Mice were injected with saline or ethanol (1.5 g/kg i.p.) and placed on an accelerating Rotarod 30 min later. Black stars indicate the effect of ethanol. $P \leq 0.001$, two-way ANOVA. (*D*) Mice were injected with ethanol (4 g/kg i.p.) and monitored until they regained their righting reflex, at which time BAL was measured. (*E*) Body temperature was measured before and after the injection of saline (triangles) or ethanol (4 g/kg i.p., circles). Black stars indicate the effect of treatment. $P \leq 0.001$, repeated-measures ANOVA. (*F*) HICs were scored before and after the injection of saline (triangles) or ethanol (4 g/kg i.p., circles). White stars indicate the effect of genotype. $P \leq 0.05$, Mann–Whitney *U* test. The effect of ethanol is described in the text. The number of mice in each subgroup is indicated on the graphs; the numbers shown in *F* apply to *E* as well. Error bars represent SEM.

GIRK3 Deletion Prevents Ethanol-Induced Activation of VTA Neurons. To further explore the role of GIRK3 in the VTA, we examined the ability of ethanol to activate VTA neurons in acutely prepared brain slices from WT and GIRK3 KO mice (23, 24). Recordings were obtained from VTA neurons displaying a stable and sustained firing rate. Single-cell reverse transcription (RT) followed by seminested PCR was conducted to determine the phenotype of a subset of VTA neurons selected using this criterion (Fig. S1). We detected TH expression in the majority of the samples (24 of 31 neurons; 77%), in accordance with the results of a previous study conducted by the same experimenter (M.A.H.) in the mouse VTA (25). The baseline firing discharge frequency of VTA neurons did not differ between WT and GIRK3 KO mice ($t_{42} = 0.3$; *P*, n.s.) (Fig. 3 *A* and *B* and Fig. S1), as reported previously (19). In addition, the firing frequency coefficient of variation and event duration were distributed similarly in WT and GIRK3 KO mice (Fig. S1). Superfusion of 25 mM ethanol did not alter VTA neuron firing in either WT or GIRK3 KO mice (Fig. 3*C* and Fig. S2); however, superfusion of 50 mM or 100 mM ethanol increased firing in WT neurons, in accordance with previous reports (26), but failed to do so in KO neurons (Fig. 3 *A* and *C* and Fig. S2). We evaluated the effect of ethanol by repeated-measures ANOVA of firing frequencies before and after ethanol superfusion, and found a significant interaction between ethanol and genotype ($F_{1,38} = 9.0$; $P \leq 0.01$). Post hoc analysis indicated that ethanol increased firing

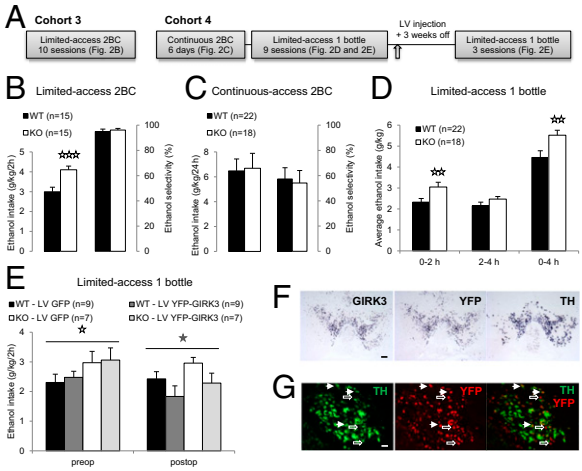

Fig. 2. Ethanol binge-like drinking on constitutive GIRK3 deletion and virally mediated expression in the VTA. (*A*) Testing timeline for results presented in *B*–*E*. (*B*) WT and GIRK3 KO mice were subjected to 2-h sessions of 2BC ethanol drinking. Average ethanol intake and preference for ethanol over the final three sessions are shown. White stars indicate the effect of genotype. $P \leq 0.001$, *t* test. (*C*) WT and GIRK3 KO mice were subjected to continuous 2BC ethanol drinking. Average ethanol intake and preference over the last 3 d are shown. (*D*) WT and GIRK3 KO mice were subjected to 4-h sessions of single-bottle ethanol drinking, and intake was measured at 2 h into the session and again at the end of the session. Average intake over the last three sessions before LV vector infusion is shown. White stars indicate the effect of genotype. $P \leq 0.01$, *t* test. (*E*) WT and GIRK3 KO mice injected with an LV vector expressing YFP-GIRK3 or GFP (negative control) in the VTA were subjected to 4-h sessions of single-bottle ethanol drinking. Average ethanol intake during the first 2 h of the session and over the last three sessions before (preoperative) and three sessions after (postoperative) LV vector infusion were analyzed separately. White stars indicate the effect of genotype. $P \leq 0.05$, two-way ANOVA. Gray stars indicate the effect of vector. $P \leq 0.05$, two-way ANOVA. The number of mice in each subgroup is indicated on the graphs. Error bars represent SEM. (*F* and *G*) Transduction of VTA neurons by the YFP-GIRK3 LV vector. (*F*) Single chromogenic in situ hybridization. GIRK3 and YFP labeling shows the area of virally mediated overexpression, which overlaps with the anatomic boundaries of the VTA highlighted by TH labeling. (Scale bar: 400 μm.) (*G*) Double-fluorescent in situ hybridization. The TH probe (green signal) labels DA neurons, and the YFP probe (red signal) labels cells expressing the transgene. The LV vector transduced both DA (white arrows) and non-DA (open arrows) cells within the VTA. (Scale bar: 50 μm.)

selectively in WT neurons ($P \leq 0.001$), whereas KO neurons were insensitive to ethanol even at the highest concentration.

GIRK3 Deletion Prevents Ethanol-Induced Release of DA in the Nucleus Accumbens. VTA DA neurons project in part to the ventral striatum, thereby forming the mesolimbic DA pathway. This neuronal circuit subserves the motivation to seek reward, and release of DA in the nucleus accumbens (NAc) on exposure to drugs of abuse is thought to encode their incentive salience (27). Thus, we hypothesized that the inability of ethanol to increase the firing of VTA neurons in GIRK3 KO mice might lead to reduced DA release in the NAc of mice receiving ethanol in vivo (28). To investigate this possibility, we used microdialysis to measure DA extracellular levels in the NAc of WT and GIRK3 KO mice (Fig. 4). Baseline NAc DA levels did not differ between GIRK3 WT and KO mice ($t_{31} = 0.6$; *P*, n.s.) (Fig. 4*A*). Ethanol (2 g/kg i.p.) increased NAc DA levels in WT mice [area under the curve AUC) = 148.0 ± 55.9; $t_{15} = 3.4$; $P \leq 0.01$], but had no effect in KO mice (AUC = −16.24 ± 72.1; $t_{16} = -0.2$; *P*, n.s.; WT vs. KO: $t_{31} = -2.5$; $P \leq 0.05$). Accordingly, repeated-measures ANOVA revealed a significant time × genotype interaction ($F_{12,372} = 2.3$; $P \leq 0.01$) (Fig. 4*B*). These results indicate that the GIRK3 subunit is critical to activation of the mesolimbic DA pathway by ethanol.

Discussion

GIRK3 deletion selectively increased ethanol binge-like drinking without affecting the sensitivity to ethanol intoxication. WT and GIRK3 KO mice metabolized ethanol at the same rate, thus ruling out the possibility that voluntary drinking increased as a result of accelerated ethanol clearance. It is noteworthy that GIRK3 deletion did not alter ethanol consumption under a continuous schedule of access or in the later part of a 4-h session. This finding points to a selective effect on drinking activity associated with intoxication (as defined by a BAL >80 mg/dL), given that continuous access to ethanol leads to sporadic bouts of drinking and produces only brief peaks of intoxication (29, 30), whereas limited access leads to binging and produces BALs that positively correlate with intake in C57BL/6J mice (31–33). Furthermore, the effect of GIRK3 deletion on binge-like drinking could be reversed by virally mediated expression of GIRK3 in the VTA, and was associated with a blunted response of the mesolimbic DA pathway to ethanol, as demonstrated by ethanol-induced excitation of VTA neurons and DA release in the NAc.

These findings suggest that the increased binge-like ethanol consumption of GIRK3 KO mice results from their insensitivity to ethanol-induced excitation of VTA DA neurons, which leads them to drink more ethanol than WT mice to achieve sufficient activation of the other neuronal circuits mediating the reinforcing effects of ethanol consumption (reviewed in ref. 34). A similar mechanism may underlie the differential ethanol intake of two mouse strains, C57BL/6J and DBA/2J. DBA/2J mice consume less ethanol than C57BL/6J mice in various ethanol self-administration paradigms, and ethanol excites VTA neurons more potently in DBA/2J mice than in C57BL/6J mice (26, 35–37). In addition, GIRK3 mRNA is expressed at higher levels in the brain, and in the midbrain in particular, of DBA/2J mice compared with C57BL/6J mice (20, 38). Overall, it appears that levels of GIRK3 expression in the VTA negatively correlate with ethanol drinking: the more GIRK3, the less ethanol consumption.

Ethanol exerts pleiotropic effects on neurotransmission and neuronal activity in the VTA. It should be noted that the concentrations of ethanol required to induce these effects are typically higher than those consistent with social drinking (e.g., 25–50 mM, with a BAL of 80 mg/dL corresponding to 17.4 mM), suggesting that the action of ethanol on the mesolimbic DA pathway only partially mediates its reinforcing effects in vivo. The net effect of ethanol on the activity of VTA DA neurons results from the summation of excitatory and inhibitory influences, including (*i*) direct excitation (23, 39); (*ii*) indirect excitation, via enhancement of glutamatergic input (40); (*iii*) disinhibition, via suppression of GABAergic input (41–43); and, in other instances, (*iv*) indirect inhibition, via enhancement of GABAergic transmission (44–47).

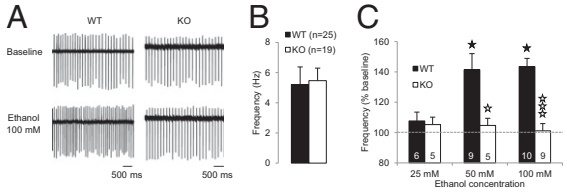

Fig. 3. Ethanol-induced excitation of VTA neurons in WT and GIRK3 KO mice. (*A*) Representative cell-attached recordings from WT (*Left*) and GIRK3 KO (*Right*) VTA neurons before (*Upper*) and during (*Lower*) superfusion of ethanol (100 mM). (Scale bar: 500 ms.) (*B*) Baseline firing frequency of WT and GIRK3 KO VTA neurons. (*C*) Ethanol-induced change in firing frequency in WT and GIRK3 KO VTA neurons. The interaction between genotype and ethanol dose was significant ($F_{2,38} = 3.9$; $P \leq 0.05$, two-way ANOVA). Post hoc analysis: black stars indicate the effect of ethanol dose (compared with 25 mM); white stars indicate the effect of genotype (one star, $P \leq 0.05$; three stars, $P \leq 0.001$). The number of mice in each group is indicated on the graph. Error bars represent SEM.

NEUROSCIENCE

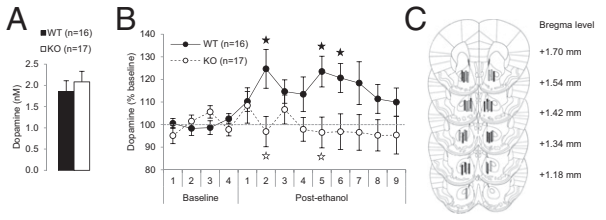

Fig. 4. Ethanol-induced release of DA in the NAc of WT and GIRK3 KO mice. (*A*) Baseline extracellular DA levels in the NAc of WT and GIRK3 KO mice. (*B*) Following a 40-min baseline period, mice were injected with ethanol (2 g/kg i.p.), and DA levels in the NAc were measured over 90 min post-injection. Samples were collected in 10-min fractions. Post hoc analysis: black stars indicate the effect of ethanol (compared with baseline); white stars indicate the effect of genotype (one star, $P \leq 0.05$). The number of mice in each group is indicated on the graph. Error bars represent SEM. (*C*) Placement of microdialysis probes targeted to the NAc of WT mice (black bars) and GIRK3 KO mice (white bars).

GIRK channels have been shown to modulate some of these effects, suggesting several ways in which the absence of GIRK3 could blunt the responsiveness of VTA DA neurons to ethanol. First, GIRK channels shape the increase in firing rate elicited by ethanol in VTA DA neurons (48). According to the mechanism proposed by McDaid et al. (48), activation of GIRK channels by ethanol produces a hyperpolarizing potential that opens hyperpolarization-activated cyclic nucleotide-gated (I_h) channels, which in turn decreases local membrane resistance and facilitates action potential generation, while simultaneously shunting the effect of the initial GIRK-dependent hyperpolarization. Thus, a reduction in I_h could decrease the response of VTA DA neurons to ethanol; however, I_h current amplitude is not altered in GIRK3 KO mice (19). Alternatively, stronger activation of GIRK channels by ethanol could counteract the depolarizing effect of I_h channels, thereby inhibiting an ethanol-induced increase in firing. This could result from enhanced surface expression of GIRK channels. Indeed, GIRK3 lacks an endoplasmic reticulum export signal and harbors a lysosomal targeting signal, two features that inhibit surface expression of GIRK3-containing tetramers (49). The peak amplitude of $GABA_B$-GIRK currents in VTA DA neurons of GIRK3 KO mice is either unchanged (19) or slightly reduced (10), however, suggesting that surface trafficking of GIRK2 homomers is not facilitated in these neurons. On the other hand, the altered subunit composition of GIRK channels expressed in GIRK3 KO mice could mediate a differential sensitivity to ethanol-induced activation. The presence of GIRK3 has been shown to reduce the coupling of $GABA_B$ receptors to GIRK channels through the selective interaction of GIRK3 with the regulator of G protein signaling 2 [RGS2 (10)], a mechanism that also could lower the sensitivity to ethanol-induced activation given the overlap between Gβγ and ethanol-binding sites (11, 12, 50).

Along similar lines, activation of GIRK channels by ethanol can potentiate $GABA_B$-mediated inhibitory postsynaptic potentials in VTA DA neurons (51). $GABA_B$ receptors on VTA DA neurons are selectively activated by GABAergic inputs from the ventral pallidum, and inhibiting these afferents increases the population activity of VTA DA neurons and DA release in the NAc (52, 53). Thus, the potentiation of $GABA_B$–GIRK coupling by ethanol would reduce VTA DA neuron firing and DA efflux in the NAc, and, as proposed above, the phenotype of GIRK3 KO mice could be explained by stronger activation of GIRK currents coupled to $GABA_B$ receptors.

Alternatively, the effect of GIRK3 deletion on ethanol-induced excitation of VTA DA neurons could be mediated by presynaptic mechanisms. GIRK channels located on presynaptic terminals have been shown to reduce GABA release onto VTA DA neurons after activation of DA D2 or $GABA_B$ receptors (54). Activation of presynaptic GIRK channels by ethanol would be expected to disinhibit VTA DA neurons, leading to an increase in VTA DA neuron firing. Thus, the hyporesponsiveness of VTA DA neurons to ethanol in GIRK3 KO mice could result from weaker activation of presynaptic GIRK channels located on GABAergic afferents. GIRK3 subunits are found in axon terminals in greater proportions than GIRK1 and GIRK2 in the hippocampus (6). If the same holds true in the VTA, then the density of GIRK channels found on GABA terminals may be lower in GIRK3 KO mice, which could underlie the reduced effect of ethanol on VTA DA neuron firing in these mice. In addition, constitutive GIRK3 deletion has been shown to down-regulate the brain-wide protein levels of GIRK1 (55). In the VTA, this effect would selectively reduce GIRK currents in GABAergic interneurons, because DA neurons do not express GIRK1 (9), and thus could diminish the ethanol-induced disinhibition of VTA DA neurons in GIRK3 KO mice.

Finally, withdrawal from repeated ethanol exposure sensitizes GIRK coupling to DA D2 receptors, thereby enhancing D2-mediated autoinhibition of VTA DA neurons, without affecting GIRK coupling to $GABA_B$ receptors (56). The resulting hypodopaminergic state could contribute to increased ethanol drinking (57, 58). This phenomenon is unlikely to underlie the binge-like drinking phenotype seen in GIRK3 KO mice, however, given that baseline VTA DA neuron activity is not altered in these mice; that is, they do not suffer from a preexisting hypodopaminergic state (19 and the present study). Moreover, increased binge-like drinking was already evident during the first sessions; that is, the GIRK3 KO phenotype did not require multiple exposures to ethanol intoxication and withdrawal.

It seems counterintuitive that constitutive deletion of GIRK3 reduces cocaine self-administration (20, 21) but increases binge-like ethanol drinking (this study). This discrepancy may result from the different sites of action of the two drugs, with cocaine acting on monoamine transporters and engaging GIRK channels downstream of monoamine signaling and ethanol acting directly on GIRK channels or engaging GIRK channels coupled to $GABA_B$ receptors, for instance (51). Thus, GIRK3-containing channels engaged by these two drugs may be located in distinct neuronal subpopulations or circuits, which could lead to divergent consequences of GIRK3 deletion on the rewarding properties of cocaine and ethanol.

Importantly, our study shows that the ability of GIRK3 to gate ethanol-induced activation of the mesolimbic DA system has functional consequences at the behavioral level, with a specific impact on binge-like drinking. This result, combined with the lack of effect of GIRK3 deletion on baseline behavior, opens up a putative avenue for curbing excessive ethanol consumption in binge drinkers without producing major side effects. The therapeutic potential of small molecules modulating the activity of GIRK channels is already being actively explored for various pathologies (reviewed in ref. 17). In particular, ML297, a compound that selectively activates GIRK1-containing heteromers, shows promising antiepileptic and anxiolytic properties while being devoid of sedative and rewarding effects (59, 60). Our present results and previous findings (15, 16) indicate that a molecule selectively targeting GIRK2/3 heteromers could be effective at blunting the reinforcing effects of ethanol. An alternative approach would be to target interaction partners that are known to regulate the G protein coupling or subcellular localization of GIRK3, such as RGS2 (10), sorting nexin 27 (22, 61, 62), neural cell adhesion molecule, or neurotrophin receptor TrkB (63). Based on the implied role of GIRK3 in the response to GHB and psychostimulants, such strategies could have benefits in the treatment of drug abuse beyond ethanol drinking (9, 10, 22).

Materials and Methods

Animals. GIRK3 KO mice were generated by homologous recombination (55) and were backcrossed onto the C57BL/6J background for more than 10 generations. WT and GIRK3 KO littermates were bred at The Scripps Research Institute in a temperature-controlled (22 °C) vivarium. Mice were maintained on a 12-h/12-h light/dark cycle. Food (standard rodent chow; Harlan Teklad) was available ad libitum at all times. Only males were used

in the experiments. Mice were at least 10 wk old when BAL time course, behavioral testing, and dialysis were performed. Mice used for electrophysiological recordings were between 8 and 10 wk old. All behavioral and dialysis experiments were conducted during the dark phase, and mice were acclimated to changes in the circadian light cycle for at least 1 wk. All procedures were carried out in accordance with the National Institutes of Health's *Guide for the Care and Use of Laboratory Animals* (64) and were approved by The Scripps Research Institute's Institutional Animal Care and Use Committee.

Ethanol Metabolism. Mice (cohort 1; WT, $n = 4$; KO, $n = 4$) were injected i.p. with 2 g/kg ethanol. Blood samples were collected from the tail vein in heparinized capillaries at 30 min, 1 h, 2 h, and 4 h postinjection. BAL was measured with an Analox Instruments GM7 analyzer.

Behavioral Testing. Three independent cohorts of mice were used in the behavioral experiments (Figs. 1*A* and 2*A*). Cohort 2 was used to assess the acute effects of ethanol (e.g., ataxia, sedation, hypothermia, handling-induced convulsions). Cohort 3 was tested in a limited-access two-bottle choice (2BC) paradigm of ethanol drinking for 10 sessions. Cohort 4 was first subjected to continuous 2BC for 6 d, and then switched to limited-access single-bottle ethanol drinking for nine sessions. These mice were then injected with LV vectors and were given 3 wk to recover before drinking sessions were resumed for three additional sessions.

For drinking experiments, 50-mL conical tubes fitted with a size 6 rubber stopper and 2.5″ stainless steel straight ball tube (Ancare) were used as bottles. Ethanol solutions were prepared with 95% ethanol (Pharmco-AAPER) and acidified water. Mice were weighed on a weekly basis to calculate ethanol intake in grams per kilogram of body weight.

Acute effects of ethanol. Mice (WT, $n = 16$; KO, $n = 16$) were first trained to balance on an accelerating rotarod for six trials (10 rpm per min acceleration; Rotarod Series 8; IITC Life Sciences). Speed at fall was recorded by a computer. Then, 2 wk later, mice were injected i.p. with 1.5 g/kg ethanol or saline (between-subject design; $n = 8$ mice of each genotype per treatment) and were retested on the accelerating Rotarod 30 min later. Speed at fall on three consecutive trials was averaged. At 2 wk later, baseline rectal body temperatures were measured using a digital thermometer (probe inserted 1.5 cm into the rectum), and baseline HICs were determined (see below). Some mice (WT, $n = 7$; KO, $n = 9$) were then injected i.p. with 4 g/kg ethanol, which resulted in the loss of righting reflex (i.e., sleeping). The time at which each mouse regained its righting reflex (i.e., ability to return to a standing position when placed on its back) was recorded, and a tail blood sample was obtained for determination of BAL at recovery. The other mice (WT, $n = 9$; KO, $n = 7$) were injected i.p. with saline. Body temperature was measured at 60 and 120 min postinjection and HICs were determined at 2, 4, 8, and 12 h postinjection in both saline- and ethanol-treated mice. HIC scoring was done on a 7-point scale ranging from facial grimace to spontaneous severe tonic-clonic convulsions (65). In brief, each mouse was picked up by the tail, and if lifting failed to elicit a convulsion, it was gently spun through a 180° arc by rubbing the tail between the thumb and forefinger.

Ethanol drinking.

Limited-access two-bottle. Mice were transferred to individual cages and offered access to two bottles, one containing ethanol (15% w:v) and the other containing water, for 2 h per day starting 3 h into the dark phase, 5 days a week (Monday through Friday). Bottles were weighed and their positions inverted daily. Mice were group-housed in their home cage and had access to a standard water bottle the rest of the time.

Continuous-access two-bottle. Mice were single-housed and were offered continuous access to two bottles, one containing ethanol (15% v:v) and the other containing water. Bottles were weighed and their positions inverted daily, Monday through Saturday, 3 h into the dark phase.

Limited-access single-bottle. Mice were single-housed and were offered access to a single bottle of ethanol (20% v:v) for 4 h per day starting 2 h into the dark phase, 3 days a week (Monday, Wednesday, and Friday). Bottles were weighed 2 h into the session and at the end of the session. A standard water bottle was available the rest of the time.

Electrophysiology.

Brain slice preparation. Brain slices containing the VTA were prepared as described previously (66) from WT ($n = 8$) and GIRK3 KO ($n = 6$) mice. In brief, mice were anesthetized (3–5% isoflurane) and promptly decapitated, and brains were placed in an ice-cold sucrose solution containing 206.0 mM sucrose, 2.5 mM KCl, 0.5 mM $CaCl_2$, 7.0 mM $MgCl_2$, 1.2 mM NaH_2PO_4, 26 mM $NaHCO_3$, 5.0 mM glucose, and 5 mM Hepes. Brains were cut into 300-μm transverse sections on a vibrating microtome (VT1000S; Leica Microsystems) and placed into oxygenated (95% O_2/5% CO_2) artificial cerebrospinal fluid (aCSF) solution composed of 130 mM NaCl, 3.5 mM KCl, 1.25 mM NaH_2PO_4, 1.5 mM $MgSO_4{\cdot}7H_2O$, 2.0 mM $CaCl_2$, 24 mM $NaHCO_3$, and 10 mM glucose. Slices were incubated in this solution for 30 min at 35–37 °C, followed by a 30-min equilibration at room temperature (21–22 °C). Following equilibration, a single slice was transferred to a recording chamber mounted on the stage of an upright microscope (Olympus BX50WI).

Recordings. VTA neurons were visualized using infrared differential interference contrast optics and an EXi Aqua camera (QImaging). A 60× magnification water immersion objective (Olympus) was used for identifying and approaching neurons. Juxtacellular (cell-attached) recordings were made with patch pipettes (3–5 MΩ; Warner Instruments) filled with aCSF coupled to a Multiclamp 700B amplifier, low-pass filtered at 2–5 kHz, digitized (Digidata 1440A digitizer), and stored on a computer using pClamp 10 software (Molecular Devices). aCSF was used as the pipette solution so as not to artificially disturb the ionic balance of the neuronal membrane (67).

Cell-attached recordings were performed in a gap-free acquisition mode with a sampling rate per signal of 10 kHz or a total data throughput equal to 20 kHz (2.29 MB/min). Neurons exhibiting stable and sustained firing were selected to test the effect of ethanol. Ethanol was prepared in aCSF and applied by bath superfusion at a final concentration of 25, 50, or 100 mM for a period of 8–10 min. The frequency of firing discharge was evaluated by threshold-based event detection analysis in Clampfit 10.2 (Molecular Devices). Event duration was determined as the time to antipeak. Baseline firing discharge was determined from a 1- to 3-min sample after stabilization, and firing discharge in the presence of ethanol was determined from a 1- to 3-min sample after full wash-in.

Microdialysis. Microdialysis evaluations of ethanol-induced increases in NAc DA levels were performed following previously described procedures (68). Data were collected from two independent cohorts (cohort 5: WT, $n = 8$; KO, $n = 9$; cohort 6: WT, $n = 8$; KO, $n = 8$) and pooled together, because there was no significant difference between baseline NAc DA level and ethanol effect for each genotype between the two cohorts. In brief, experimentally naïve mice were implanted stereotaxically with microdialysis probes with a 1-mm active membrane length localized in the NAc (relative to bregma: +1.5 mm AP, ±0.8 mm ML, and -5.0 mm V from skull) (69). After at least 12 h of postimplantation, equilibration dialysate samples were collected at 10-min intervals using an aCSF perfusate (149 mM NaCl, 2.8 mM KCl, 1.2 mM $CaCl_2$, 1.2 mM $MgCl_2$, 0.25 mM ascorbate, and 5.4 mM D-glucose; pH 7.2–7.4) delivered at 0.6 μL/min. Samples were collected during a 40-min baseline period and for 90 min after a 2-g/kg i.p. ethanol challenge. This ethanol dose results in intoxicating BALs during ∼3 h postinjection (Fig. 1*B*). On collection, each sample was immediately frozen and subsequently stored at −80 °C. Dialysate DA content was quantified using HPLCy coupled with electrochemical detection (model HTEC-500; EiCOM) as described previously (68).

LV Vector Injection, In Situ Hybridization, Single-Cell RT-PCR, and Data Analysis. These procedures are described in detail in *SI Text* and Fig. S3.

ACKNOWLEDGMENTS. We thank Dr. George Koob for his valuable and constructive recommendations on this project, Dr. Nicolas Grillet for his expert guidance with in situ hybridization, and Dr. Nicholas Gilpin for his help with statistical analysis. This work was supported by National Institutes of Health Grants AA020913 (to C.C.), AA018734 (to P.A.S.), DA034696 (to K.W.), MH061933 (to K.W.), AA020430 (to M.A.H.), AA013498 (to M.R.), AA020404 (to L.H.P.), and AA006420 (to C.C., L.H.P., and M.R.).

1. Lüscher C, Slesinger PA (2010) Emerging roles for G protein-gated inwardly rectifying potassium (GIRK) channels in health and disease. *Nat Rev Neurosci* 11(5): 301–315.
2. Karschin C, Dissmann E, Stühmer W, Karschin A (1996) IRK(1-3) and GIRK(1-4) inwardly rectifying K^+ channel mRNAs are differentially expressed in the adult rat brain. *J Neurosci* 16(11):3559–3570.
3. Grosse G, et al. (2003) Axonal sorting of Kir3.3 defines a GABA-containing neuron in the CA3 region of rodent hippocampus. *Mol Cell Neurosci* 24(3):709–724.
4. Koyrakh L, et al. (2005) Molecular and cellular diversity of neuronal G-protein–gated potassium channels. *J Neurosci* 25(49):11468–11478.
5. Aguado C, et al. (2008) Cell type-specific subunit composition of G protein-gated potassium channels in the cerebellum. *J Neurochem* 105(2):497–511.
6. Fernández-Alacid L, Watanabe M, Molnár E, Wickman K, Luján R (2011) Developmental regulation of G protein-gated inwardly-rectifying K^+ (GIRK/Kir3) channel subunits in the brain. *Eur J Neurosci* 34(11):1724–1736.
7. Inanobe A, et al. (1999) Characterization of G-protein–gated K^+ channels composed of Kir3.2 subunits in dopaminergic neurons of the substantia nigra. *J Neurosci* 19(3):1006–1017.
8. Jelacic TM, Kennedy ME, Wickman K, Clapham DE (2000) Functional and biochemical evidence for G-protein–gated inwardly rectifying K^+ (GIRK) channels composed of GIRK2 and GIRK3. *J Biol Chem* 275(46):36211–36216.

9. Cruz HG, et al. (2004) Bi-directional effects of GABA(B) receptor agonists on the mesolimbic dopamine system. *Nat Neurosci* 7(2):153–159.
10. Labouèbe G, et al. (2007) RGS2 modulates coupling between GABAB receptors and GIRK channels in dopamine neurons of the ventral tegmental area. *Nat Neurosci* 10(12):1559–1568.
11. Aryal P, Dvir H, Choe S, Slesinger PA (2009) A discrete alcohol pocket involved in GIRK channel activation. *Nat Neurosci* 12(8):988–995.
12. Bodhinathan K, Slesinger PA (2013) Molecular mechanism underlying ethanol activation of G-protein–gated inwardly rectifying potassium channels. *Proc Natl Acad Sci USA* 110(45):18309–18314.
13. Kobayashi T, et al. (1999) Ethanol opens G-protein–activated inwardly rectifying K^+ channels. *Nat Neurosci* 2(12):1091–1097.
14. Lewohl JM, et al. (1999) G-protein–coupled inwardly rectifying potassium channels are targets of alcohol action. *Nat Neurosci* 2(12):1084–1090.
15. Hill KG, Alva H, Blednov YA, Cunningham CL (2003) Reduced ethanol-induced conditioned taste aversion and conditioned place preference in GIRK2 null mutant mice. *Psychopharmacology (Berl)* 169(1):108–114.
16. Blednov YA, Stoffel M, Chang SR, Harris RA (2001) Potassium channels as targets for ethanol: Studies of G-protein–coupled inwardly rectifying potassium channel 2 (GIRK2) null mutant mice. *J Pharmacol Exp Ther* 298(2):521–530.
17. Luján R, Marron Fernandez de Velasco E, Aguado C, Wickman K (2014) New insights into the therapeutic potential of Girk channels. *Trends Neurosci* 37(1):20–29.
18. Pravetoni M, Wickman K (2008) Behavioral characterization of mice lacking GIRK/Kir3 channel subunits. *Genes Brain Behav* 7(5):523–531.
19. Arora D, et al. (2010) Altered neurotransmission in the mesolimbic reward system of Girk mice. *J Neurochem* 114(5):1487–1497.
20. Kozell LB, Walter NA, Milner LC, Wickman K, Buck KJ (2009) Mapping a barbiturate withdrawal locus to a 0.44-Mb interval and analysis of a novel null mutant identify a role for Kcnj9 (GIRK3) in withdrawal from pentobarbital, zolpidem, and ethanol. *J Neurosci* 29(37):11662–11673.
21. Morgan AD, Carroll ME, Loth AK, Stoffel M, Wickman K (2003) Decreased cocaine self-administration in Kir3 potassium channel subunit knockout mice. *Neuropsychopharmacology* 28(5):932–938.
22. Munoz MB, Slesinger PA (2014) Sorting nexin 27 regulation of G protein-gated inwardly rectifying K^+ channels attenuates in vivo cocaine response. *Neuron* 82(3): 659–669.
23. Brodie MS, Shefner SA, Dunwiddie TV (1990) Ethanol increases the firing rate of dopamine neurons of the rat ventral tegmental area in vitro. *Brain Res* 508(1):65–69.
24. Gessa GL, Muntoni F, Collu M, Vargiu L, Mereu G (1985) Low doses of ethanol activate dopaminergic neurons in the ventral tegmental area. *Brain Res* 348(1):201–203.
25. Grieder TE, et al. (2014) VTA CRF neurons mediate the aversive effects of nicotine withdrawal and promote intake escalation. *Nat Neurosci* 17(12):1751–1758.
26. Brodie MS, Appel SB (2000) Dopaminergic neurons in the ventral tegmental area of C57BL/6J and DBA/2J mice differ in sensitivity to ethanol excitation. *Alcohol Clin Exp Res* 24(7):1120–1124.
27. Berridge KC (2007) The debate over dopamine's role in reward: The case for incentive salience. *Psychopharmacology (Berl)* 191(3):391–431.
28. Di Chiara G, Imperato A (1988) Drugs abused by humans preferentially increase synaptic dopamine concentrations in the mesolimbic system of freely moving rats. *Proc Natl Acad Sci USA* 85(14):5274–5278.
29. Dole VP, Gentry RT (1984) Toward an analogue of alcoholism in mice: Scale factors in the model. *Proc Natl Acad Sci USA* 81(11):3543–3546.
30. Kreifeldt M, Le D, Treistman SN, Koob GF, Contet C (2013) BK channel β1 and β4 auxiliary subunits exert opposite influences on escalated ethanol drinking in dependent mice. *Front Integr Neurosci* 7:105.
31. Becker HC, Lopez MF (2004) Increased ethanol drinking after repeated chronic ethanol exposure and withdrawal experience in C57BL/6 mice. *Alcohol Clin Exp Res* 28(12):1829–1838.
32. Contet C, et al. (2014) μ-Opioid receptors mediate the effects of chronic ethanol binge drinking on the hippocampal neurogenic niche. *Addict Biol* 19(5):770–780.
33. Rhodes JS, Best K, Belknap JK, Finn DA, Crabbe JC (2005) Evaluation of a simple model of ethanol drinking to intoxication in C57BL/6J mice. *Physiol Behav* 84(1):53–63.
34. Koob GF, Volkow ND (2010) Neurocircuitry of addiction. *Neuropsychopharmacology* 35(1):217–238.
35. Belknap JK, Crabbe JC, Young ER (1993) Voluntary consumption of ethanol in 15 inbred mouse strains. *Psychopharmacology (Berl)* 112(4):503–510.
36. Grahame NJ, Cunningham CL (1997) Intravenous ethanol self-administration in C57BL/6J and DBA/2J mice. *Alcohol Clin Exp Res* 21(1):56–62.
37. Rhodes JS, et al. (2007) Mouse inbred strain differences in ethanol drinking to intoxication. *Genes Brain Behav* 6(1):1–18.
38. Smith SB, et al. (2008) Quantitative trait locus and computational mapping identifies Kcnj9 (GIRK3) as a candidate gene affecting analgesia from multiple drug classes. *Pharmacogenet Genomics* 18(3):231–241.
39. Brodie MS, Pesold C, Appel SB (1999) Ethanol directly excites dopaminergic ventral tegmental area reward neurons. *Alcohol Clin Exp Res* 23(11):1848–1852.
40. Xiao C, et al. (2009) Ethanol facilitates glutamatergic transmission to dopamine neurons in the ventral tegmental area. *Neuropsychopharmacology* 34(2):307–318.
41. Gallegos RA, Lee RS, Criado JR, Henriksen SJ, Steffensen SC (1999) Adaptive responses of gamma-aminobutyric acid neurons in the ventral tegmental area to chronic ethanol. *J Pharmacol Exp Ther* 291(3):1045–1053.
42. Stobbs SH, et al. (2004) Ethanol suppression of ventral tegmental area GABA neuron electrical transmission involves *N*-methyl-D-aspartate receptors. *J Pharmacol Exp Ther* 311(1):282–289.
43. Xiao C, Zhang J, Krnjević K, Ye JH (2007) Effects of ethanol on midbrain neurons: Role of opioid receptors. *Alcohol Clin Exp Res* 31(7):1106–1113.
44. Guan Y, et al. (2012) GABAergic actions mediate opposite ethanol effects on dopaminergic neurons in the anterior and posterior ventral tegmental area. *J Pharmacol Exp Ther* 341(1):33–42.
45. Melis M, Camarini R, Ungless MA, Bonci A (2002) Long-lasting potentiation of GABAergic synapses in dopamine neurons after a single in vivo ethanol exposure. *J Neurosci* 22(6): 2074–2082.
46. Theile JW, Morikawa H, Gonzales RA, Morrisett RA (2008) Ethanol enhances GABAergic transmission onto dopamine neurons in the ventral tegmental area of the rat. *Alcohol Clin Exp Res* 32(6):1040–1048.
47. Theile JW, Morikawa H, Gonzales RA, Morrisett RA (2011) GABAergic transmission modulates ethanol excitation of ventral tegmental area dopamine neurons. *Neuroscience* 172:94–103.
48. McDaid J, McElvain MA, Brodie MS (2008) Ethanol effects on dopaminergic ventral tegmental area neurons during block of Ih: Involvement of barium-sensitive potassium currents. *J Neurophysiol* 100(3):1202–1210.
49. Ma D, et al. (2002) Diverse trafficking patterns due to multiple traffic motifs in G protein-activated inwardly rectifying potassium channels from brain and heart. *Neuron* 33(5):715–729.
50. Whorton MR, MacKinnon R (2013) X-ray structure of the mammalian GIRK2-βγ G-protein complex. *Nature* 498(7453):190–197.
51. Federici M, Nisticò R, Giustizieri M, Bernardi G, Mercuri NB (2009) Ethanol enhances GABAB-mediated inhibitory postsynaptic transmission on rat midbrain dopaminergic neurons by facilitating GIRK currents. *Eur J Neurosci* 29(7):1369–1377.
52. Floresco SB, West AR, Ash B, Moore H, Grace AA (2003) Afferent modulation of dopamine neuron firing differentially regulates tonic and phasic dopamine transmission. *Nat Neurosci* 6(9):968–973.
53. Sugita S, Johnson SW, North RA (1992) Synaptic inputs to GABAA and GABAB receptors originate from discrete afferent neurons. *Neurosci Lett* 134(2):207–211.
54. Michaeli A, Yaka R (2010) Dopamine inhibits GABA(A) currents in ventral tegmental area dopamine neurons via activation of presynaptic G-protein coupled inwardly-rectifying potassium channels. *Neuroscience* 165(4):1159–1169.
55. Torrecilla M, et al. (2002) G-protein-gated potassium channels containing Kir3.2 and Kir3.3 subunits mediate the acute inhibitory effects of opioids on locus ceruleus neurons. *J Neurosci* 22(11):4328–4334.
56. Perra S, Clements MA, Bernier BE, Morikawa H (2011) In vivo ethanol experience increases D(2) autoinhibition in the ventral tegmental area. *Neuropsychopharmacology* 36(5): 993–1002.
57. George SR, et al. (1995) Low endogenous dopamine function in brain predisposes to high alcohol preference and consumption: Reversal by increasing synaptic dopamine. *J Pharmacol Exp Ther* 273(1):373–379.
58. Melis M, Spiga S, Diana M (2005) The dopamine hypothesis of drug addiction: Hypodopaminergic state. *Int Rev Neurobiol* 63:101–154.
59. Kaufmann K, et al. (2013) ML297 (VU0456810), the first potent and selective activator of the GIRK potassium channel, displays antiepileptic properties in mice. *ACS Chem Neurosci* 4(9):1278–1286.
60. Wydeven N, et al. (2014) Mechanisms underlying the activation of G-protein–gated inwardly rectifying K^+ (GIRK) channels by the novel anxiolytic drug, ML297. *Proc Natl Acad Sci USA* 111(29):10755–10760.
61. Balana B, et al. (2011) Mechanism underlying selective regulation of G protein-gated inwardly rectifying potassium channels by the psychostimulant-sensitive sorting nexin 27. *Proc Natl Acad Sci USA* 108(14):5831–5836.
62. Lunn ML, et al. (2007) A unique sorting nexin regulates trafficking of potassium channels via a PDZ domain interaction. *Nat Neurosci* 10(10):1249–1259.
63. Kleene R, et al. (2010) Functional consequences of the interactions among the neural cell adhesion molecule NCAM, the receptor tyrosine kinase TrkB, and the inwardly rectifying K^+ channel KIR3.3. *J Biol Chem* 285(37):28968–28979.
64. National Research Council (2011) *Guide for the Care and Use of Laboratory Animals* (The National Academies Press, Washington, DC), 8th Ed.
65. Crabbe JC, Merrill C, Belknap JK (1991) Acute dependence on depressant drugs is determined by common genes in mice. *J Pharmacol Exp Ther* 257(2):663–667.
66. Nimitvilai S, et al. (2014) Dopamine D2 receptor desensitization by dopamine or corticotropin-releasing factor in ventral tegmental area neurons is associated with increased glutamate release. *Neuropharmacology* 82:28–40.
67. Alcami P, Franconville R, Llano I, Marty A (2012) Measuring the firing rate of high-resistance neurons with cell-attached recording. *J Neurosci* 32(9):3118–3130.
68. Ramchandani VA, et al. (2011) A genetic determinant of the striatal dopamine response to alcohol in men. *Mol Psychiatry* 16(8):809–817.
69. Franklin KBJ, Paxinos G (2008) *The Mouse Brain in Stereotaxic Coordinates* (Academic, San Diego), Compact 3rd Ed.